Flux Measurements, Flux Estimation Techniques, and Fine-Scale Turbulence Measurements in the Unstable Surface Layer Over Land

F. H. CHAMPAGNE, C. A. FRIEHE[1] AND J. C. LARUE

Department of Applied Mechanics and Engineering Sciences, University of California-San Diego, La Jolla 92093

J. C. WYNGAARD

Cooperative Institute for Research in Environmental Sciences, University of Colorado/NOAA, Boulder 80307 and Wave Propagation Laboratory, NOAA, Boulder 80302

(Manuscript received 21 May 1976, in revised form 12 November 1976)

ABSTRACT

An AFCRL-UCSD joint experiment in Minnesota in 1973 has provided a comparison of direct and indirect measurements of the surface-layer fluxes of momentum, heat and moisture under unstable conditions. The direct momentum and heat flux measurements of the two groups agreed well, and also agreed well with values inferred by the direct dissipation technique. The moisture flux estimates from the inertial-dissipation technique also agreed well with the directly measured values.

Several of the important terms in the budgets of turbulent kinetic energy and turbulent scalar variances were evaluated directly. The imbalance (or pressure transport) term in the energy budget was estimated, and the ratio of the imbalance term to the dissipation term determined from the present experiment agrees well with the Kansas results. The dissipation rate of temperature variance exceeded its production rate, in contrast with the Kansas results, implying an imbalanced temperature variance budget. Several possible contributors to this imbalance are discussed.

The one-dimensional spectra of the temperature and streamwise velocity fluctuations are presented in Kolmogorov normalized form. Spectral moments to fourth order are shown to agree with earlier results. Values of the universal velocity and temperature spectral constants of $\alpha_1=0.50\pm0.02$ and $\beta_\theta=0.45\pm0.02$ were obtained.

1. Introduction

The turbulent fluxes of momentum, heat and moisture in the atmospheric surface layer are important to many aspects of meteorology and oceanography. Consequently, the surface layer has been studied in some detail, with emphasis on understanding turbulent transport processes under a wide range of stability conditions and on developing instrumentation and techniques to determine the turbulent fluxes. For a review of experimental methods used in atmospheric boundary layer studies, see *Atmospheric Technology*, No. 7, 1975.

There are several methods for determining surface layer fluxes, including the direct covariance method which requires the measurement of the covariance of the turbulent variables, and the profile, inertial-dissipation and direct dissipation rate techniques where the fluxes are obtained indirectly, using measurements of related statistical quantities. The direct covariance method, while straightforward, generally requires the use of expensive equipment to obtain accurate measurements. In ship or aircraft applications, instrument platform motion can severely contaminate the velocity signals, thereby degrading the flux measurements. Correction for this contamination is extremely difficult since it requires precise, simultaneous measurement of the instrument platform motion (see Kaimal and Haugen, 1969).

The dissipation rate techniques are much less sensitive to instrument platform motion. The measurement of the dissipation rates of the turbulent velocity, temperature and humidity fields can be made at frequencies much higher than those of the platform motion so that contamination is minimized. The dissipation rate measurements are obtained either from spectral density or structure function data in the inertial subrange of frequency or spatial separation (the inertial-dissipation technique), or by direct measurement of the derivative statistics which define the dissipation rates (the direct dissipation technique). The turbulent fluxes are then estimated through the use of the budget equations for the turbulent kinetic energy, temperature variance and humidity variance, as discussed in detail later.

Here we present results for momentum, heat and

[1] Also Scripps Institution of Oceanography.

moisture fluxes obtained by direct and indirect techniques, as well as turbulent fine-structure revealed in the process of direct dissipation measurements.

2. Flux determination techniques

a. The direct covariance method

The vertical fluxes of momentum, sensible heat and moisture are defined by

$$\left.\begin{aligned} \tau &= -\rho\overline{uw} = \rho u_*^2 \\ H &= \rho c_p \overline{w\theta} = -\rho c_p u_* T_* \\ E &= \overline{wq} = -u_* q_* \end{aligned}\right\}, \tag{1}$$

where u and w are the streamwise horizontal and the vertical velocity fluctuations, θ is the temperature fluctuation, q the humidity[2] fluctuation, ρ air density, c_p specific heat at constant pressure u_* the friction velocity, T_* and q_* the temperature and humidity scales, respectively, and the overbar denotes a time average.

In the direct covariance method one forms the instantaneous product of the vertical velocity with the variable of interest and averages the result. The covariances $\overline{uw}$, $\overline{w\theta}$ and $\overline{wq}$ are also integrals of their respective cospectra over frequency. The bandwidth required to measure the entire $\overline{uw}$ cospectrum, for example, is typically on the order of $10^{-3} \leqslant fz/U \leqslant 10$, where f is frequency (Hz), z the height above the surface, and U the mean wind speed (see McBean, 1972).

b. Inertial-dissipation technique

This method, apparently first proposed by Deacon (1959) and demonstrated by Taylor (1961), has been applied by many investigators to the surface layer over the ocean. These include Smith (1967), Weiler and Burling (1967), Miyake *et al.* (1970), Smith (1970), Pond *et al.* (1971), Hicks and Dyer (1972), Stegen *et al.* (1973), Dyer (1975), and Leavitt and Paulson (1975). In the earlier works, neutral, locally isotropic, horizontally homogeneous, stationary surface-layer turbulence was usually assumed, with a kinetic energy balance

$$-\overline{uw}\frac{\partial U}{\partial z} = \epsilon, \tag{2}$$

where the first term represents shear production and ϵ is the rate of dissipation of turbulent kinetic energy. Under the assumed conditions, we have

$$\frac{\partial U}{\partial z} = \frac{u_*}{\kappa z}, \tag{3}$$

where κ is von Kármán's constant. Combining Eqs. (2) and (3) yields

$$u_*^2 = -\overline{uw} = (\kappa\epsilon z)^{\frac{2}{3}}. \tag{4}$$

The value of ϵ can be determined from a measurement of the one-dimensional velocity spectrum in the inertial subrange, i.e.,

$$\varphi_{uu}(k_1) = \alpha_1 \epsilon^{\frac{2}{3}} k_1^{-5/3}, \quad \overline{u^2} = \int_0^\infty \varphi_{uu}(k_1)dk_1, \tag{5}$$

where α_1 is the one-dimensional Kolmogorov constant, assumed known, and k_1 is the wavenumber obtained from the cyclic frequency f using Taylor's approximation (see Taylor, 1938, and Lumley, 1965), $k_1 = 2\pi f U^{-1}$. Equivalently, Taylor (1961) determined ϵ from the second-order structure function in the inertial subrange, i.e.,

$$D_{uu}(r) = \overline{[u(x+r)-u(x)]^2} = 4.02\alpha_1 \epsilon^{\frac{2}{3}} r^{\frac{2}{3}}, \tag{6}$$

where r is the magnitude of the separation vector.

Thus, from Eq. (4), the momentum flux under neutral conditions can be estimated using ϵ obtained from Eqs. (5) or (6). Away from neutral, however, the effects of stability on the mean profiles and on the turbulent energy budget should be considered.

The budget of the turbulent kinetic energy, $\frac{1}{2}\overline{e^2} = \frac{1}{2}(\overline{u^2}+\overline{v^2}+\overline{w^2})$, simplifies under the assumptions of horizontal homogeneity and stationarity to

$$-\overline{uw}\frac{\partial U}{\partial z} + \frac{g}{T_v}(\overline{w\theta}+0.61T\overline{wm}) - \frac{1}{2}\frac{\partial}{\partial z}\overline{we^2} - \frac{1}{\rho}\frac{\partial}{\partial z}\overline{pw} - \epsilon = 0, \tag{7}$$

where $T_v = T(1+0.61M)$ is the virtual temperature, T is the mean absolute temperature, m the fluctuating specific humidity,[3] M the mean specific humidity and p the pressure fluctuation. The terms in Eq. (7) represent, respectively, the shear production, buoyant production (including the effect of humidity fluctuations), divergence of the turbulent flux of kinetic energy, divergence of the pressure-velocity covariance or pressure transport, and dissipation. Under unstable conditions, many investigators (see Busch and Panofsky, 1968; Pond *et al.*, 1971; McBean *et al.*, 1971; Hicks and Dyer, 1972) have approximated (7) by

$$-\overline{uw}\frac{\partial U}{\partial z} + \frac{g}{T_v}(\overline{w\theta}+0.61T\overline{wm}) - \epsilon = 0, \tag{8}$$

which states that total production balances dissipation.

---

[2] Precisely, q is water vapor density or absolute humidity (g m^{-3}).

[3] The specific humidity m is related to q by $m = 7.735\times10^{-4} Tq/273$, where the units of m are grams of water vapor per gram of moist air, those of q are grams of water vapor per cubic meter of moist air, and T is in kelvins.

An extensive and systematic investigation of the energy budget was carried out during the 1968 AFCRL Kansas experiment (Haugen *et al.*, 1971; Wyngaard and Coté, 1971). All terms except pressure transport were measured, and the dissipation rate ϵ was obtained from hot-wire anemometer measurements extending over the dissipative range. Wyngaard and Coté (1971) concluded from their analysis of the Kansas data that the buoyant production and the flux divergence terms are approximately in balance for the stability range $-1\leqslant z/L\leqslant 0$ so a better budget approximation than Eq. (8), at least for the over-land case, is

$$\overline{uw}\frac{\partial U}{\partial z}+\epsilon+I=0, \tag{9}$$

where I is the measured imbalance, a substantial gain term under unstable conditions. They suggested that this imbalance could be attributed to the only unmeasured term, pressure transport. A recent attempt to measure pressure transport directly by McBean and Elliott (1975; see also Elliott, 1975) gave general agreement with Wyngaard and Coté's conclusion. The empirical expression for the imbalance term given by Wyngaard and Coté (1971) is

$$\frac{\kappa z}{u_*^3}I=(1-15z/L)^{-\frac{1}{4}}-(1+0.5|z/L|^{\frac{2}{3}})^{\frac{3}{4}}, \tag{10}$$

where L is the Monin-Obukhov length scale defined as

$$L=[-u_*^3T_v/\kappa g(\overline{w\theta}+0.61T\overline{wm})]. \tag{11}$$

Mean profiles are also strongly affected by stability. Dyer (1967) and Businger *et al.* (1971) found that under unstable conditions Eq. (3) is invalid, and instead

$$\varphi_M\left(\frac{z}{L}\right)=\frac{\kappa z}{u_*}\frac{\partial U}{\partial z}=(1-15z/L)^{-\frac{1}{4}}. \tag{12}$$

The history of indirect flux measurement techniques presents a rather confused picture. Various expressions for the mean profiles and for the turbulent energy budget have been used. Further, stability effects have not always been consistently included, and various values have been used for the Kolmogorov and von Kármán constants. Possibly because of compensating errors, however, some of these earlier attempts have been fairly successful. For estimating the momentum fluxes from the slightly unstable BOMEX data, Pond *et al.* (1971) used Eq. (8), $\alpha_1=0.55$, and the logarithmic-profile form Eq. (3). Their results exhibit considerable scatter but appear to compare favorably with the directly computed flux values. They neglected the effects of stability on the velocity profile, although not on the scalar profile, as they obtained better results in doing so. Hicks and Dyer (1972) used Eqs. (5), (8) and (12) to estimate the momentum flux over land and suggest the same for the surface layer over water. They concluded that their estimates of the momentum flux were adequate using a value of α_1 of 0.54, but pointed out the need for further investigation.

Until further results concerning the energy budget become available, it would seem preferable to use Eq. (9) along with Eqs. (10) and (12) to estimate the momentum flux under unstable conditions by the inertial dissipation technique. Combining these equations gives

$$u_*=\left[\frac{\kappa z\epsilon}{(1+0.5|z/L|^{\frac{2}{3}})^{\frac{3}{2}}}\right]^{\frac{1}{3}}. \tag{13}$$

Note that the presence of the stability-dependent term introduces further complications in that the sensible heat and moisture fluxes must be known to estimate the momentum flux. This means the state of stability of the surface layer must be established to determine the fluxes.

The budget equations for the scalar variances under stationary, horizontally homogeneous conditions are

$$-2\overline{w\theta}\frac{\partial T}{\partial z}-\frac{\partial}{\partial z}\overline{w\theta^2}=\chi_\theta, \tag{14}$$

$$-2\overline{wq}\frac{\partial Q}{\partial z}-\frac{\partial}{\partial z}\overline{wq^2}=\chi_q, \tag{15}$$

where Q is the mean humidity (g m^{-3}), and χ_θ and χ_q are the temperature variance and humidity variance dissipation rates, respectively. Note that the scalar variance equations (14) and (15) are written for the budgets of $\overline{\theta^2}$ and $\overline{q^2}$ rather than $\frac{1}{2}\overline{\theta^2}$ and $\frac{1}{2}\overline{q^2}$. The first term in each equation is the rate of production by interaction of the vertical turbulent flux with the mean scalar gradient. The second and third terms in each equation represent the divergence of the vertical flux of scalar variance and the rate of destruction by molecular diffusivity, respectively.

There have been fewer experimental studies of the scalar variance budget equations than of the kinetic energy budget equation. Wyngaard and Coté did not measure χ_θ, but found that the flux divergence term for temperature variance averaged about -5% of the production term in the unstable range $-1\leqslant z/L\leqslant 0$. Thus

$$\chi_\theta=-2\overline{w\theta}\frac{\partial T}{\partial z}. \tag{16}$$

This gave values of the Kolmogorov inertial subrange constant β_θ, where

$$\varphi_{\theta\theta}(k_1)=\beta_\theta\chi_\theta\epsilon^{-\frac{1}{3}}k_1^{-5/3},\ \overline{\theta^2}=\int_0^\infty\varphi_{\theta\theta}(k_1)dk_1, \tag{17}$$

which agreed with most of the data available then.

Monji (1973) also found Eq. (16) to be valid over land [χ_θ was inferred from inertial subrange spectral measurements using Eq. (17)], and observed that the flux divergence term changed sign for $z/L<-1$, as did Wyngaard and Coté. Garratt (1972), from data taken over the surface of a lake, also found that production essentially balanced estimated dissipation. In all the referenced studies of the $\overline{\theta^2}$ budget the value of χ_θ was not directly measured but was inferred from Eq. (17) using a β_θ value of 0.4. Recent measurement of β_θ obtained over land by Williams (1974) and those reported herein are not significantly different and do not alter any of the conclusions reached in the referenced studies. Therefore, Eq. (16) will be considered a valid approximation for the temperature variance budget.

The Kansas result for the mean temperature gradient is (Businger *et al.*, 1971)

$$\varphi_T\left(\frac{z}{L}\right)=\frac{\kappa z}{T_*}\frac{dT}{dz}=\frac{1}{\alpha_T}\left(1-9\frac{z}{L}\right)^{-\frac{1}{2}} \tag{18}$$

for unstable conditions, where α_T is the ratio of eddy transfer coefficients for heat and momentum. They found that for neutral conditions $\alpha_T=1.35$ and also $\kappa=0.35$, rather than the traditional value of 0.40. Combining (16) and (18) gives an expression for T_*,

$$T_*=-\left(\frac{\kappa z\chi_\theta}{2u_*\varphi_T}\right)^{\frac{1}{2}}, \tag{19}$$

where the negative root is taken for the unstable conditions considered here. Since the right side depends on the stability of the surface layer, to obtain the desired estimate of the sensible heat flux we need to determine L and χ_θ. The latter can be obtained from spectral measurements in the inertial subrange and Eq. (17), while the former requires knowledge of the momentum and moisture fluxes.

The humidity variance budget is not as well-documented as those for the kinetic energy and temperature variance, primarily because moisture statistics are more difficult to measure (see Kaimal, 1975), and it is not presently possible to measure directly the dissipation rate χ_q. Some studies have been made over the open ocean (Pond *et al.*, 1971; Leavitt and Paulson, 1975), and based on those results we will assume that the humidity budget is similar to that for the temperature variance, so that

$$\chi_q=-2\overline{wq}\frac{\partial Q}{\partial z}. \tag{20}$$

Values of χ_q are determined from inertial range spectral measurements using

$$\varphi_{qq}(k_1)=\beta_q\chi_q\epsilon^{-\frac{1}{3}}k_1^{-5/3}, \quad \overline{q^2}=\int_0^\infty \varphi_{qq}(k_1)dk_1, \tag{21}$$

where β_q is assumed to be known. Since there are no direct measurements of β_q, it is usually assumed equal to β_θ. Paquin and Pond (1971) estimated β_θ and β_q from second- and third-order structure functions and found $\beta_\theta=\beta_q\approx 0.4$.

The mean humidity gradient is assumed to be given by

$$\varphi_q\left(\frac{z}{L}\right)=\frac{\kappa z}{q_*}\frac{\partial Q}{\partial z}=\frac{1}{\alpha_q}\left(1-9\frac{z}{L}\right)^{-\frac{1}{2}}, \tag{22}$$

similar to Eq. (18) for temperature, and further α_q is assumed equal to α_T. Eqs. (20) and (22) can be combined to give

$$q_*=-\left(\frac{\kappa z\chi_q}{2u_*\varphi_q}\right)^{\frac{1}{2}}, \tag{23}$$

so that both χ_q and L are required to estimate the moisture flux. Again, the negative root is taken for conditions with positive (upward) moisture fluxes.

Pond *et al.* (1971) used the inertial dissipation technique to estimate the scalar fluxes for BOMEX and San Diego data. In general, the estimates of the sensible heat flux from this technique were considerably higher (at times by a factor of 2 or more) than direct measurements, while the moisture flux estimates showed good agreement with their directly measured values. Hicks and Dyer (1972), from a similar study over land, concluded that the inertial dissipation technique provided adequate estimates for the sensible heat flux using a value of $2\beta_\theta$ of 0.71. Moisture effects were neglected.

In the inertial-dissipation technique, the dissipation rates ϵ, χ_θ and χ_q are obtained from spectral measurements of the appropriate variable in the inertial range of wavenumbers. An alternative is to measure these dissipation rates directly, as discussed in the next section.

c. *The direct dissipation technique*

Pond *et al.* (1963) and Gibson and Williams (1969) demonstrated that ϵ may be measured directly in the atmospheric boundary layer. Gibson *et al.* (1970) measured ϵ directly during project BOMEX and extended the technique to measure χ_θ. Invoking the assumption of local isotropy and using Taylor's hypothesis, the expressions for ϵ and χ_θ can be written

$$\epsilon=15\nu\overline{\left(\frac{\partial u}{\partial x}\right)^2}=\frac{15\nu}{U^2}\overline{\left(\frac{\partial u}{\partial t}\right)^2}, \tag{24}$$

$$\chi_\theta=6\mathfrak{D}\overline{\left(\frac{\partial\theta}{\partial x}\right)^2}=\frac{6\mathfrak{D}}{U^2}\overline{\left(\frac{\partial\theta}{\partial t}\right)^2}, \tag{25}$$

where $\mathfrak{D}$ is the molecular diffusivity for temperature. Measurements of the variances of the time derivatives of u and θ require spatial resolution of the sensing

probes to nearly the Kolmogorov scale $\eta=(\nu^3/\epsilon)^{\frac{1}{4}}$ (typically about 1 mm in atmospheric flows), correspondingly high-frequency response of the associated circuitry and sensors, and good signal-to-noise ratios.

Heskestad (1965) and Lumley (1965) have shown that this use of Taylor's hypothesis overestimates ϵ in high-intensity turbulence. Lumley's fluctuating convection velocity model gives

$$\overline{\left(\frac{\partial u}{\partial t}\right)^2}=U^2\overline{\left(\frac{\partial u}{\partial x}\right)^2}\left(1+\frac{\overline{u^2}}{U^2}+2\frac{\overline{v^2}+\overline{w^2}}{U^2}\right), \tag{26}$$

which is equivalent to Eq. (24) only in low-intensity flows. Heskestad also obtained Eq. (26), but in a completely different way. He squared and averaged the Navier-Stokes equation for u, assuming local isotropy and that velocity and velocity derivative fluctuations are uncorrelated.

We extended the Heskestad model to a scalar and obtained [in agreement with the extension of Lumley's model by Wyngaard and Clifford (1976)]

$$\overline{\left(\frac{\partial\theta}{\partial t}\right)^2}=U^2\overline{\left(\frac{\partial\theta}{\partial x}\right)^2}\left(1+\frac{\overline{u^2}+\overline{v^2}+\overline{w^2}}{U^2}\right). \tag{27}$$

Thus we can rewrite (24) and (25) as

$$\epsilon=15\nu\overline{\left(\frac{\partial u}{\partial x}\right)^2}=\frac{15\nu}{U^2}\overline{\left(\frac{\partial u}{\partial t}\right)^2}\left(1+\frac{\overline{u^2}}{U^2}+2\frac{\overline{v^2}+\overline{w^2}}{U^2}\right)^{-1}, \tag{28}$$

$$\chi_\theta=6\mathfrak{D}\overline{\left(\frac{\partial\theta}{\partial x}\right)^2}=\frac{6\mathfrak{D}}{U^2}\overline{\left(\frac{\partial\theta}{\partial t}\right)^2}\left(1+\frac{\overline{u^2}+\overline{v^2}+\overline{w^2}}{U^2}\right)^{-1}. \tag{29}$$

Eqs. (28) and (29) were used to calculate ϵ and χ_θ. The values averaged 16% and 10% less than those indicated by Eqs. (24) and (25).

Stegen *et al.* (1973) compared momentum and sensible heat flux measurements from the direct dissipation technique with results from the direct covariance and inertial dissipation techniques obtained by other investigators during BOMEX. In general the comparisons were encouraging with the exception of the high estimates of the sensible heat flux inferred from the inertial dissipation technique using $\beta_\theta=0.4$.

d. Computation of fluxes

We now have relations for u_*, q_* and T_* in terms of the measured dissipation rates and stability-dependent terms. The latter pose complications by coupling the equations and no simple, direct solution is possible. A solution procedure, however, was developed by combining the relevant equations for u_*, T_*, q_* and L such that an expression relating the measured quantities as a function of z/L was obtained. Hicks and Dyer (1972) used a similar procedure but they neglected humidity effects in their equations, often a good approximation over land but not in the marine boundary layer. The desired expression, including humidity effects, can be obtained as follows.

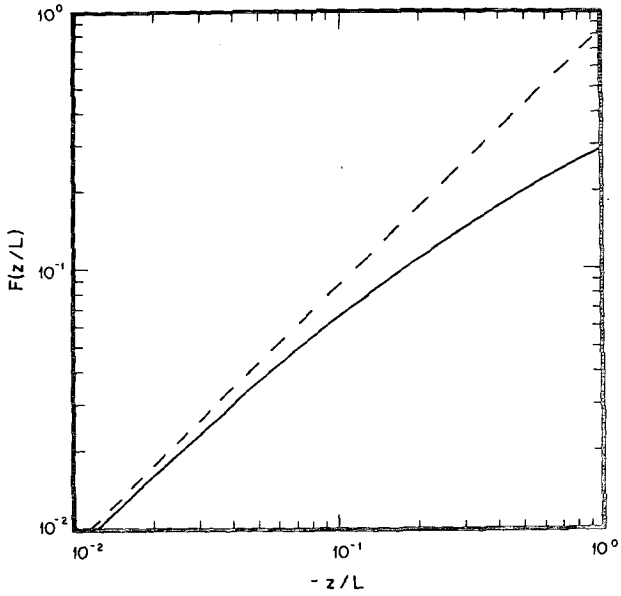

FIG. 1. The function $F(z/L)$ from Eq. (31) (solid) Eq. (32) (dashed).

Eq. (11) may be written in the form

$$L=\frac{-u_*^3\left[1+0.472\times10^{-3}\left(\frac{T}{273}\right)Q\right]}{\kappa g\left[\frac{\overline{w\theta}}{T}+0.472\times10^{-3}\left(\frac{T}{273}\right)\overline{wq}\right]}. \tag{30}$$

Substituting the equations for u_*, T_* and q_* into Eq. (30) gives, after some manipulation,

$$\frac{(\kappa z\chi_\theta)^{\frac{1}{2}}\kappa zg\left[\frac{1}{T}+0.472\times10^{-3}\frac{T}{273}\left(\frac{\chi_q}{\chi_\theta}\right)^{\frac{1}{2}}\right]}{\sqrt{2}(\kappa z\epsilon)^{5/6}[1+0.472\times10^{-3}(T/273)Q]}$$

$$=\frac{-\frac{z}{L}\left[\frac{1}{\alpha_T}\left(1-9\frac{z}{L}\right)^{-\frac{1}{2}}\right]^{\frac{1}{2}}}{[1+0.5|z/L|^{\frac{3}{4}}]^{5/4}}=F(z/L). \tag{31}$$

Values of $F(z/L)$ have been computed using $\alpha_T=\alpha_q=1.35$ with the result shown in Fig. 1. Estimates of the fluxes can be obtained by first determining the value of $F(z/L)$ from the measured quantities ϵ, χ_θ, χ_q, T, Q and z, then determining z/L from Eq. (31) or Fig. 1, and finally computing u_*, T_* and q_* from Eqs. (13), (19) and (23), respectively, as the stability terms are now determined. The effect of the mean humidity can

normally be neglected as it changes the value of $F(z/L)$ by less than 1% for typical boundary layer conditions.

The z/L terms appearing in the brackets on the right side of Eq. (31) arise from the stability dependence of the imbalance term I and the generalized gradients ϕ_M and ϕ_T. If the imbalance term is set to zero and stability effects are not considered, as was originally done in the development of the dissipation technique, $F(z/L)$ becomes

$$F(z/L)=-\frac{1}{\sqrt{\alpha_T}}\frac{z}{L}. \tag{32}$$

Eq. (32) is also plotted on Fig. 1 to show that stability effects and inclusion of the imbalance term are significant for even near-neutral conditions. At $F(z/L)=0.1$, $z/L=-0.15$ from Eq. (32), whereas Eq. (31) gives -0.18; under more unstable conditions the discrepancy becomes much larger.

3. Experimental details

a. Site

Greater upper Minnesota was the location of the boundary layer experiment described here. A large section of farmland in the Red River Valley of the North (48°34′N, 96°52′W) was specially prepared for the experiment, with a plowed soil surface with furrows approximately 20 cm deep and 40 cm apart, running east to west. The desired wind direction was from the north, and the fetch was uniform in this direction for several kilometers upwind of the instrument towers; the soil was plowed only about 25 m to the south of the towers. The surface was very flat, with a few shallow large-scale undulations, estimated at approximately 50 cm in height over horizontal distances of ~0.3 km. The soil was a dense black mixture of silt and clay, known locally as "gumbo."

Boundary layer observations reported herein were made simultaneously by the AFCRL and UCSD groups during the afternoon of 28 September 1973. The wind was from the north, and the sky was clear with a few scattered low clouds. Several days of intermittent heavy showers preceded that day and the soil was well-saturated, with only a few areas of standing water evident.

The AFCRL and UCSD instrument towers were located at the southern edge of the field, approximately 100 m apart in the east-west direction. The 32 m AFCRL tower had turbulence instrumentation at 4 and 32 m. The UCSD instrumentation was placed on mounting brackets on top of two 4 m, 5 cm diameter guyed poles. Turbulence instrumentation was on one pole, and monitoring instrumentation (cup anemometer, cooled-mirror aspirated dew-point unit) was on the other pole, 7 m away to avoid interference.

b. Instrumentation

1) Low frequency

The AFCRL instrumentation is described in detail in papers covering other aspects of this field program (Readings *et al.*, 1974; Kaimal *et al.*, 1976). Here we mention only the relevant 4 m instrumentation, an EG&G Model 198-3 sonic anemometer and a Cambridge Systems platinum resistance thermometer.

UCSD low-frequency turbulence instrumentation consisted of an EG&G Model 198 sonic anemometer, a platinum resistance thermometer and a Lyman-alpha humidiometer. The UCSD sonic anemometer was directly calibrated in the UCSD low-speed wind tunnel prior to the field experiment. The calibration revealed that there was a slight distortion of the array due to misalignment of the vertical path, but this was accounted for in the subsequent data analysis. The fluctuating water vapor density was measured with an ERC Model B Lyman-alpha humidiometer. The device was calibrated in a Cambridge Systems hygrometric facility at the Naval Undersea Center, San Diego, prior to the field experiment. Calibration was also obtained *in situ* from the EG&G Model 110S(M) dewpoint unit. The bandwidth of the Lyman-alpha device appears to be dc to ~10 Hz. The exponential response of the instrument to humidity was accounted for in the digital analysis of the data. The temperature signal required for direct computation of the sensible heat flux was obtained by low-pass filtering the high-frequency temperature signal, which is discussed in the following section.

2) High frequency

High-frequency measurements of the turbulent streamwise velocity component were obtained using a DISA 55M01 (constant temperature anemometer) and 55D10 (linearizer) system. A DISA 55F11 tungsten hotwire probe was used (5 μm diameter by 1.0 mm length), operated at an overheat ratio of 1.8 (210 K). Frequency response, with a 50 m probe cable, was measured to be ~18 kHz at a calibration velocity of 7 m s^{-1} using the square wave response technique. The temperature sensitivity was estimated and found to have a negligible contribution to the reported statistics. The anemometer system was calibrated at the field site prior to and after the experimental run. The hotwire sensor was in the horizontal plane, perpendicular to the mean flow direction.

Temperature fluctuations were measured with a resistance platinum thermometer (0.62 μm diameter by 0.65 mm length) which was formed from an etched section of Wollaston wire which was mounted on a Thermo-Systems 1210 probe. The sensor was operated in an ac Wheatstone bridge circuit designed by T. K. Deaton. Current through the 210 Ω wire was 255 μA rms. Bandwidth of a sensor of the above dimensions

and operated at the conditions of the experiment is estimated to be dc to approximately 2 kHz (LaRue *et al.*, 1975). Calibration of the fluctuating temperature signal was obtained by modulating the current through the sensor such that the output voltage change corresponded to 1.00 K (assuming a value of 0.0034 K^{-1} for the temperature-resistance coefficient for platinum). The velocity sensitivity of the sensor is estimated to be 1.4×10^{-2} K m^{-1} s and is neglected (Wyngaard, 1972; LaRue *et al.*, 1975).

c. *Data analysis*

1) SIGNAL PROCESSING

Signals were recorded digitally by AFCRL, and in analog form by UCSD. The AFCRL data acquisition system is described by Kaimal (1975). The analog signals from the UCSD instrumentation were preconditioned before being recorded on an FM tape recorder (Honeywell 7610, operated at 15 inches per second, bandwidth dc to 5 kHz), in order to use its dynamic range optimally. Amplitude levels were recovered on playback to within $\pm1\%$ over the range dc to 5 kHz.

For some portions of the data analysis, the time derivatives of u and θ were required. These were obtained with an analog differentiator and low-pass filter combination having unity gain at 15.9 Hz and bandwidth dc to 10 kHz.

2) DATA SELECTION

From the several hours of data recorded, approximately 1 h was selected for detailed analysis. The period analyzed corresponded in time to 1544 to 1644 CST on 28 September 1973. During that period the wind was from the north and constant in speed and direction. There was, however, a small decrease with time of the sensible heat flux in the period. For this reason, and also to correspond with the standard AFCRL 15 min analysis period, the 1 h period was separated into four sections of about 15 min each which are designated as Runs 1, 2, 3 and 4.

3) DATA REDUCTION

The recorded signals were digitized in the laboratory at UCSD using a 12-bit resolution analog-to-digital converter with sample-and-hold circuits and a multiplexer for multi-channel analysis. The low-frequency signals of u, w, θ and q were sampled at 16.28 per second, while $\partial u/\partial t$ and $\partial\theta/\partial t$ were sampled at two rates (4170 and 521 s^{-1}) in order to give good spectral resolution from dc to ~2 kHz. Data reduction was performed on the UCSD CDC 3600 computer using statistical and spectral programs developed at UCSD. The fluxes were computed directly from the simultaneously-sampled (16.28 s^{-1}) time series of u, w, θ and q. To reduce the effects of nonstationarity and ultra-low-frequency fluctuations, the fluxes were computed from the ensemble averages of the covariances computed from fluctuations about 63 s means.

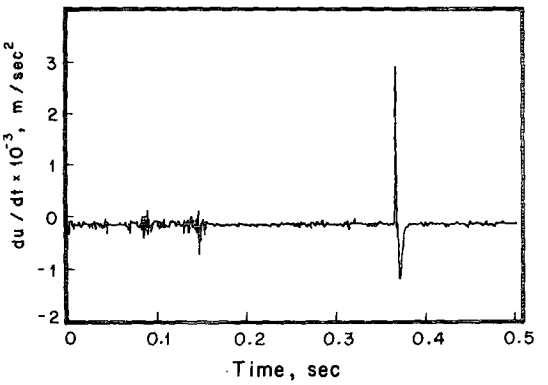

FIG. 2. Digital time series of a record of the velocity derivative $\partial u/\partial t$ showing the characteristic large spike at approximately 0.375 s. It is believed that the spike is caused by a particle striking the hot-wire anemometer probe.

The dissipation rates of velocity and temperature were obtained from the variances of the 4170 s^{-1} digitized time series. The skewness and kurtosis values were also routinely calculated, and it was observed that the velocity derivative data in a few records (typically 10 out of the 1800 per run) contributed enormously to these higher moments. These records gave velocity derivative kurtosis values greater than 100, with maximum values of about 2000. For the velocity derivative signal, time series plots of these records revealed a characteristic asymmetric large amplitude spike, as shown in Fig. 2. It is believed that this spike signal is the result of the anemometer circuit responding to a small particle striking the active section of the hot-wire probe. The records with extremely large (>100) kurtosis values were deleted for the final calculation of the velocity statistics. No such characteristic spikes were found in the temperature derivative signal. However, since the temperature and velocity derivative signals were sampled simultaneously, the same temperature derivative records were dropped; these deletions caused less than 2% changes in the variances of $\partial u/\partial t$ and $\partial\theta/\partial t$.

The power spectra of the velocity and temperature derivative signals were obtained using a fast Fourier transform routine on the 4170 and 521 Hz sampled data. The resulting spectra were combined and smoothed with a 9-point running average, to cover the range 0.25 to 2086 Hz.

4. Results and discussion

a. *Spectra*

Since the flux estimation techniques require values for the dissipation rates as input, some of the measured

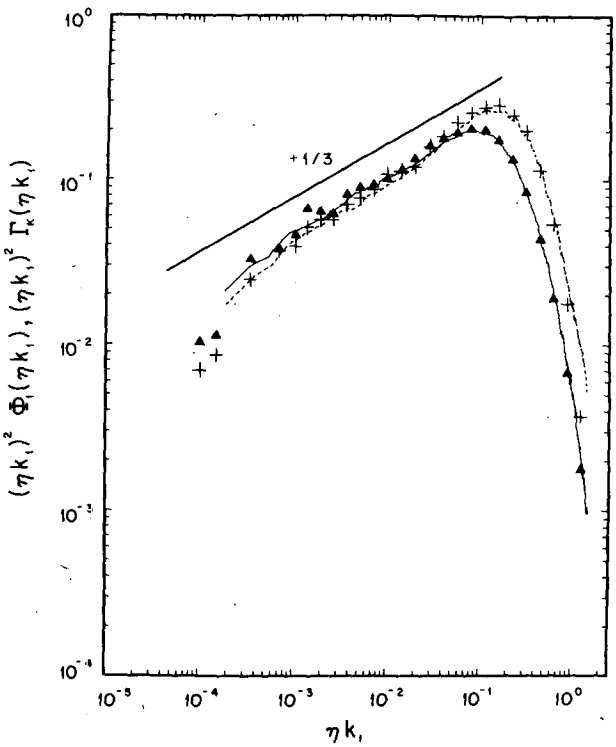

FIG. 3. Normalized velocity derivative and temperature derivative spectra. Run 1: $\dot{u}$ (solid), $\dot{\theta}$ (dashed); Williams: $\dot{u}$ (▲ ▲), $\dot{\theta}$ (+ +).

spectra will be presented to demonstrate the capability and limitations of the instrumentation used. The one-dimensional spectra of the derivatives $\partial u/\partial x$ and $\partial\theta/\partial x$ from Run 1 are presented in Fig. 3 in Kolmogorov-normalized form defined by

$$(\eta k_1)^2\Phi_{11}(\eta k_1)=\frac{\nu^{\frac{1}{4}}}{\epsilon^{\frac{1}{4}}}k_1^2\varphi_{uu}(k_1), \tag{33}$$

$$(\eta k_1)^2\Gamma_K(\eta k_1)=\frac{(\nu\epsilon)^{\frac{1}{4}}}{\chi_\theta}k_1^2\varphi_{\theta\theta}(k_1), \tag{34}$$

where $\Phi_{11}(\eta k_1)$ and $\Gamma_K(\eta k_1)$ are the Kolmogorov-normalized spectrum functions. An inertial subrange appears to exist for more than one decade in wavenumber as apparent from the agreement with a $+\frac{1}{3}$ slope, indicated by the solid straight line. Also shown for comparison are the surface-layer data of Williams (1974) for both temperature and velocity, which show good agreement with the present data. The dissipation rates ϵ and χ_θ in (33) and (34) were determined from the second moments of the spectra through the isotropic relations

$$\epsilon=15\nu\int_0^\infty k_1^2\varphi_{uu}(k_1)dk_1, \tag{35}$$

$$\chi_\theta=6\mathfrak{D}\int_0^\infty k_1^2\varphi_{\theta\theta}(k_1)dk_1. \tag{36}$$

Note that ϵ and χ_θ from (35) and (36) differ from the corrected values given by (28) and (29). It was necessary to use the uncorrected values here to permit comparison of the spectra with earlier results.

Fig. 4 shows the normalized derivative spectra on a linear-linear plot. The Kolmogorov frequency, i.e., the frequency corresponding to $\eta k_1=1$, was 1370 Hz for our data. Since the frequency response of the hot-wire anemometer was 17 kHz and that of the cold wire 2 kHz, the bandwidth of the instrumentation was adequate for determination of ϵ and χ_θ.

The length of the hot wire was $l_w=1$ mm, corresponding to $\eta/l_w=0.68$. Its spatial resolution was adequate since, according to Wyngaard's (1968) analysis, the spectral attenuation is less than 10% at $\eta k_1=1$ and causes no significant underestimate in ϵ (see Wyngaard, 1969). Similar results apply for the cold wire which was 0.65 mm in length (Wyngaard, 1971).

The tail of the normalized temperature spectrum does not approach the abscissa in Fig. 4 asymptotically because of noise in the ac bridge and associated circuitry. The effects of noise are probably insignificant until $\eta k_1>0.6$, as can be inferred from Fig. 5 which shows the fourth moments of the normalized spectra. The approximate normalized wavenumber for which the signal-to-noise ratio is unity is 1.0 for temperature and 1.3 for velocity. The low-pass filters used in data playback and digitizing were set at 2000 Hz or at $\eta k_1=1.46$. Thus the contribution of noise to the value of χ_θ is less than a few percent, while that to ϵ is negligible.

The magnitude and position of the peak values of the second- and fourth-moment curves for the normalized velocity spectrum agree well with those of Williams (1974) and of Wyngaard and Pao (1971). These results demonstrate that high quality spectral data were obtained for both velocity and temperature.

Values of the "universal constants" α_1 and β_θ were obtained as shown in Fig. 6. This linear-log plot allows closer examination of the data for inertial subrange behavior, since a straight line fit to the data in the inertial subrange region should have zero slope. For the wavenumber range $1\times10^{-3}<\eta k_1<2\times10^{-2}$ apparent inertial subranges exist for both u and θ with the measured values $\alpha_1=0.46\pm0.02$ and $\beta_\theta=0.40\pm0.02$. Williams' data are also presented in Fig. 6 and agree quite favorably with our own. Both sets of normalized temperature spectral data exhibit an unexpected bump or relative peak near $\eta k_1=0.1$. No plausible theoretical explanation for the bump has yet been obtained.

Taylor's (1938) "frozen-flow" approximation was used to convert frequency to wavenumber in the spectral analysis. This breaks down in high-intensity turbulence, leading to underestimates of α_1 (Lumley, 1965) and β_θ (Wyngaard and Clifford, 1976). Our corrected values are $\alpha_1=0.50\pm0.02$ and $\beta_\theta=0.41\pm0.02$. The failure of Taylor's approximation also distorts

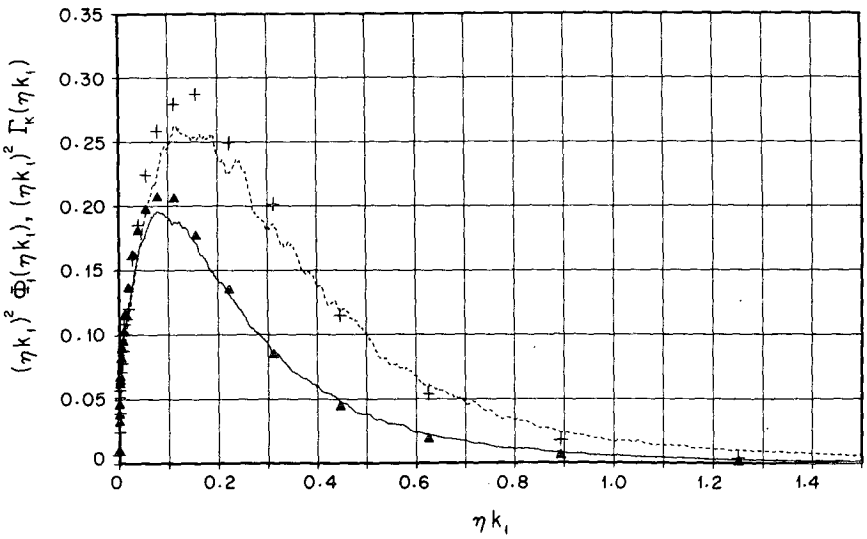

FIG. 4. Normalized velocity derivative and temperature derivative spectra. Symbols as in Fig. 3.

high-wavenumber spectra, as will be shown in a forthcoming paper by Champagne *et al.*, but we have done no more than correct α_1 and β_θ here.

Another interesting feature of the Kolmogorov-normalized velocity and temperature spectra plots is the significantly greater spectral content in the normalized temperature spectrum for $\eta k_1 > 0.06$ than in the normalized velocity spectrum. This is at least partly due to the different relations between three-dimensional and one-dimensional spectra for velocity and temperature, i.e.,

$$\varphi_{uu}(k_1) = \int_{k_1}^{\infty} \left(1 - \frac{k_1^2}{k^2}\right) \frac{E(k)}{k}\, dk, \tag{37}$$

$$\varphi_{\theta\theta}(k_1) = \int_{k_1}^{\infty} \frac{F(k)}{k}\, dk, \tag{38}$$

respectively. Here E and F are the three-dimensional velocity and temperature spectra (Hinze, 1959). If the same forms are used for E and F, the one-dimensional spectra will differ because of the differences in the integrals in (37) and (38). We used the Corrsin (1964) and Pao (1965) three-dimensional spectral expression and numerically integrated to obtain Kolmogorov-normalized one-dimensional spectra. Their relative shapes were similar to the data (but there was no bump), with more content in the scalar spectrum at high wavenumbers.

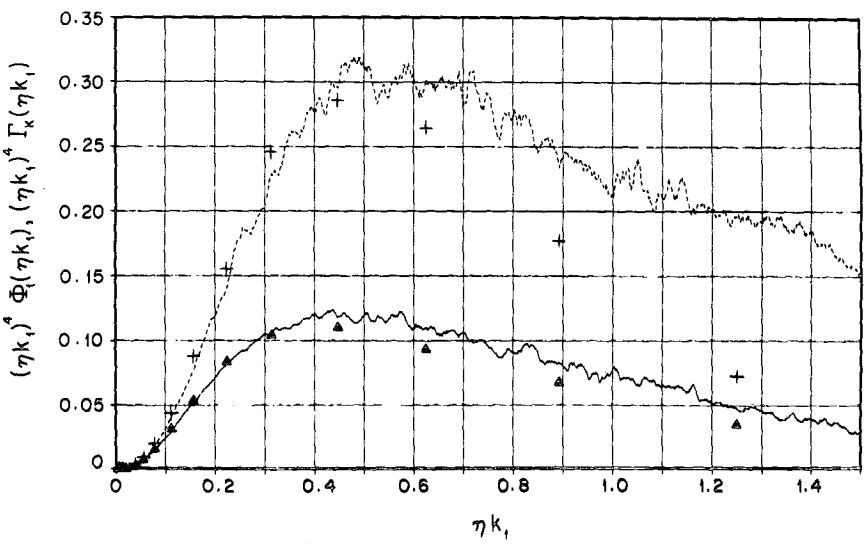

FIG. 5. Fourth moments of normalized velocity and temperature spectra. Symbols as in Fig. 3.

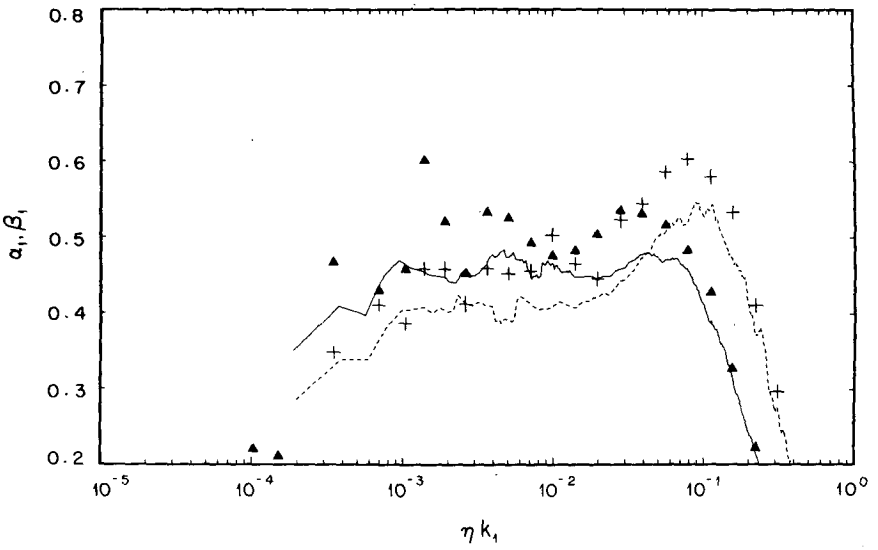

FIG. 6. Universal constants α_1 and β_θ. Run 1: α_1 (solid), β_θ (dashed); Williams: α_1(▲▲), β_θ(++). This is a plot of $(\eta k_1)^{5/3}$ times the power spectra and represents α_1 and β_θ only in the inertial subrange.

The measurement of the humidity fluctuations was limited by instrumentation response and resolution problems. The spatial separation of the Lyman-alpha detector and source tube was about 1.0 cm, which corresponds roughly to a frequency of 90 Hz for winds of 5.5 m s^{-1}. Evidently flow blockage or other effects limit the effective upper frequency to roughly 10 Hz.

The humidity spectrum for Run 1 is shown in Fig. 7. The spike at 60 Hz is caused by line noise. From the velocity and temperature spectral data, an inertial subrange in the humidity spectrum would be expected between frequencies of 1 to about 28 Hz. Fig. 7 indicates the start of an apparent inertial subrange around 1 Hz, and it appears to terminate near 8 Hz; but this roll-off is probably due to the response of the humidiometer. From the spectral level at 1 Hz, the value of χ_q was estimated using Eq. (21) with $\beta_q=0.05$.

b. The fluxes

The mean conditions, turbulence levels and dissipation rates for Runs 1–4 are presented in Table 1. Fig. 8

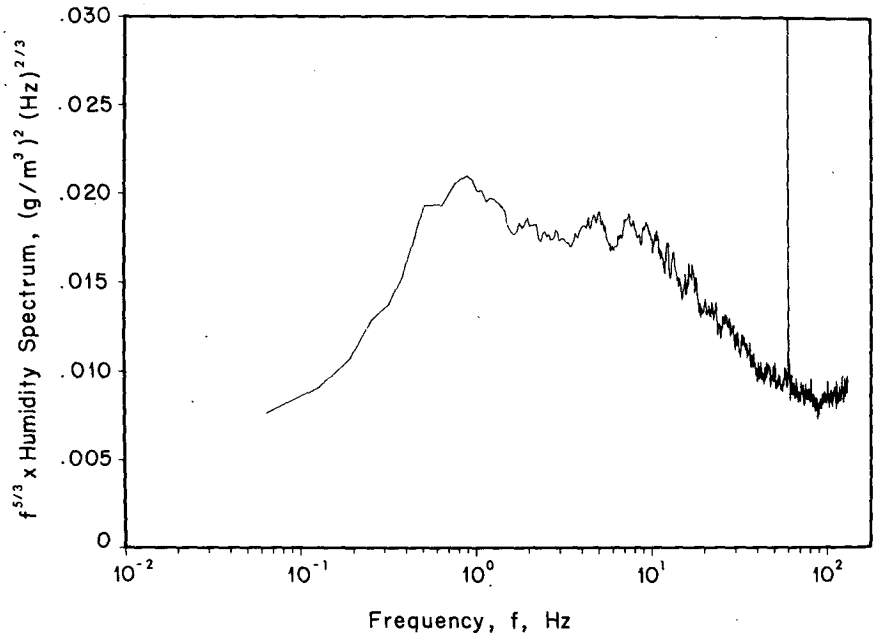

FIG. 7. Semi-logarithmic plot of the 5/3 moment of the humidity spectrum. The spike at 60 Hz is due to line noise pickup.

TABLE 1. Experiment conditions and dissipation rate values.[a]

Run	U (m s^{-1})	T (°C)	Q (g m^{-3})	$\overline{u^2}^{\frac{1}{2}}$ (m s^{-1})	$\overline{w^2}^{\frac{1}{2}}$ (m s^{-1})	$\overline{v^2}^{\frac{1}{2}}$ (m s^{-1})	$\overline{\theta^2}^{\frac{1}{2}}$ (K)	$\overline{q^2}^{\frac{1}{2}}$ (g m^{-3})	ϵ (10^2 m^2 s^{-3})	χ_θ (10^3 K^2 s^{-1})	χ_q (10^2 g^2 m^{-6} s^{-1})
1	5.48	23.0	9.4	0.94	0.38	1.59	0.32	0.47	1.94	6.41	1.18
2	5.28	23.1	9.4	0.97	0.39	1.28	0.27	0.48	1.65	3.82	1.10
3	6.21	23.2	9.3	1.20	0.43	1.35	0.19	0.45	1.99	2.18	1.10
4	5.67	23.2	9.3	1.05	0.44	1.49	0.18	0.39	2.32	2.33	0.91

[a] Values of ν and $\mathfrak{D}$ used were $\nu=0.159$ cm^2 s^{-1}, $\mathfrak{D}=0.219$ cm^2 s^{-1}, Pr$=0.725$. Mean pressure was 28.84 inches Hg.

presents the directly measured turbulent shear stress values and the values estimated by the direct dissipation technique. The length of the horizontal bars represents the time period over which the average was obtained. The UCSD directly computed results are generally higher by 10–15% than those of AFCRL, and this appears to be a general trend rather than scatter.

The directly computed $\overline{w\theta}$ and the estimated values are presented in Fig. 9. The UCSD and AFCRL directly computed values agree quite well, but the values estimated from the direct dissipation technique are consistently high. Also shown in Fig. 9 are the UCSD directly computed $\overline{wq}$ values and the indirect values, which show good agreement, on average. Table 2 presents the UCSD directly computed covariances and the values estimated by the dissipation technique.

c. *The variance budgets*

The directly measured values of $\overline{uw}$, $\overline{w\theta}$, $\overline{wq}$, ϵ and χ_θ and the estimated χ_q provide sufficient information to evaluate several of the important terms in the three variance budgets. The mean gradient terms necessary for the various production terms were determined from the Businger *et al.* (1971) relationships using the measured values of z/L_m, where L_m denotes the value of L obtained from the directly measured covariances.

1) THE TURBULENT KINETIC ENERGY BUDGET

The turbulent kinetic energy equation (7) can be made dimensionless through multiplication by $-\kappa z/u_*^3$ to obtain

$$\varphi_M\frac{z}{L}-\frac{1}{2}\frac{\kappa z}{u_*^3}\frac{\partial}{\partial z}\overline{we^2}-\frac{\kappa z}{u_*^3}I-\frac{\kappa z\epsilon}{u_*^3}=0, \qquad (39)$$

where I, the imbalance term, is assumed to be pressure transport. Table 3 presents the various terms computed from the direct measurements: I_m/ϵ is the measured imbalance, as defined by Eq. (9), normalized by the measured dissipation rate; and $(I/\epsilon)_w$ is the same

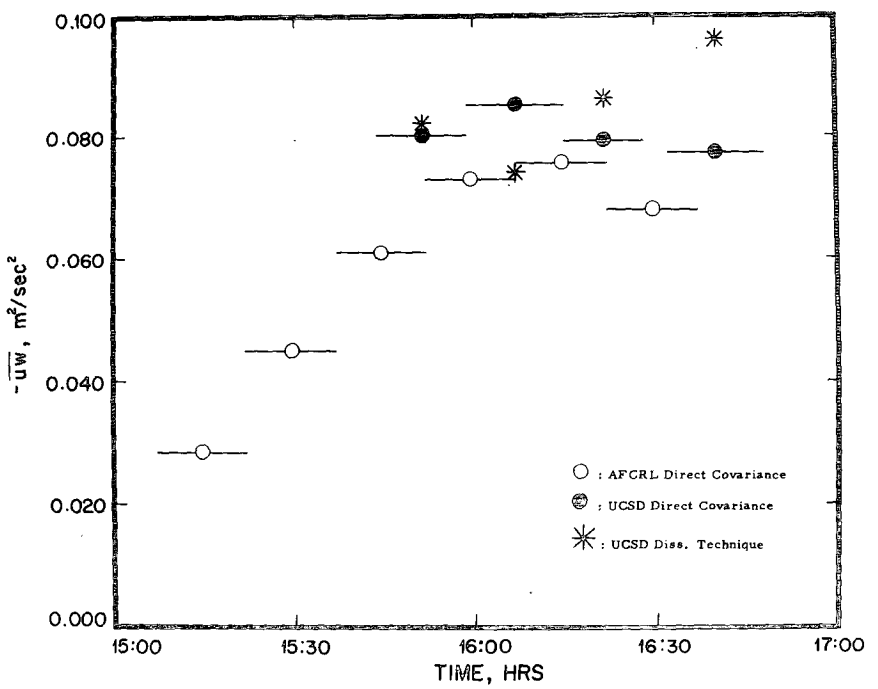

FIG. 8. Values of the turbulent shear stress during the experiment. The length of the horizontal bar is the averaging time.

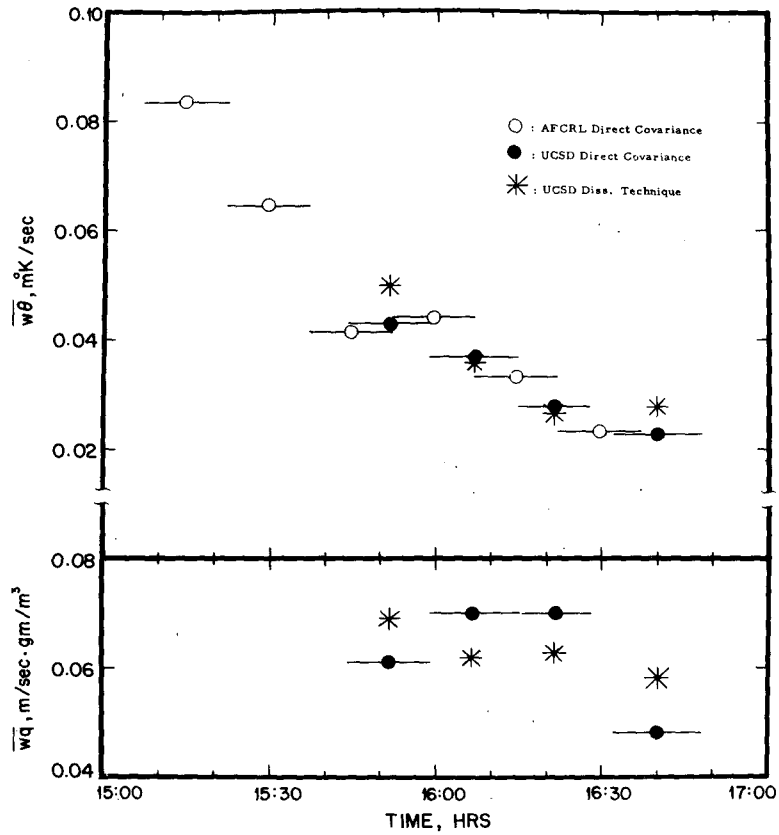

FIG. 9. Values of the turbulent fluxes of temperature and moisture during the experiment. Symbols as in Fig. 8

variable computed from Wyngaard and Coté's (1971) results, which can be expressed as

$$\left(\frac{I}{\epsilon}\right)_W = \frac{[1-15(z/L)]^{-\frac{1}{4}}}{[1+0.5|z/L|^{\frac{2}{3}}]^{\frac{3}{2}}} - 1.0, \qquad (40)$$

where the measured L values were used for computation. The values presented in Table 3 are shown in Fig. 10 together with the results of Wyngaard and Coté (1971). The agreement is good over the limited range of z/L for the present data. The scatter in the directly measured values of ϵ perhaps can be attributed to the difficulty of measuring the variance of the signal $\partial u/\partial t$ which has a large kurtosis (Tennekes and Wyngaard, 1972).

2) THE SCALAR VARIANCE BUDGETS

The production, dissipation and flux divergence terms for the scalar variance budgets are presented in Tables 4 and 5. The flux divergence terms were esti-

TABLE 2. Summary of results.

	$-\overline{uw}$ (m² s⁻²)			$\overline{w\theta}$ (m° K s⁻¹)			$\overline{wq}$ (g m⁻² s⁻¹)					
Run	Direct	Dissipation[a]	Error[b] (%)	Direct	Dissipation[a]	Error[b] (%)	Direct	Dissipation[c]	Error[b] (%)	L_θ (m)	L_q (m)	L_m[d] (m)
1	0.080	0.082	+3	0.043	0.051	+18	0.061	0.069	+13	−45.2	−210	−37.2
2	0.085	0.074	−13	0.037	0.038	+3	0.070	0.064	−9	−57.6	−204	−44.9
3	0.079	0.086	+9	0.028	0.028	+0	0.070	0.063	−10	−69.4	−180	−50.1
4	0.077	0.096	+25	0.023	0.029	+26	0.048	0.058	+21	−79.8	−257	−60.9
Average	0.080	0.084	+6	0.033	0.036	+12	0.062	0.063	+2		—	

[a] Direct dissipation technique.
[b] Error = 10^2 (dissipation − direct)/direct.
[c] Inertial dissipation technique.
[d] $L_m = (L_\theta^{-1} + L_q^{-1})^{-1}$, where L_θ is the Monin-Obukhov length due to sensible heat flux and L_q the Monin-Obukhov length due to moisture flux, from directly measured fluxes.

TABLE 3. Dimensionless kinetic energy budget terms, including measured and estimated imbalance term.

Run	φ_M	$-z/L_m$	$\frac{\kappa z}{u_*^3} I_m$ [a]	$\frac{\kappa z \epsilon}{u_*^3}$	$\frac{I_m}{\epsilon}$	$\left(\frac{I}{\epsilon}\right)_w$ [b]
1	0.783	0.110	−0.442	1.226	−0.36	−0.33
2	0.805	0.091	−0.144	0.949	−0.15	−0.30
3	0.819	0.082	−0.465	1.284	−0.36	−0.29
4	0.842	0.067	−0.721	1.563	−0.46	−0.25
Average	0.812	0.088	−0.443	1.255	−0.33	−0.30

[a] Eq. (9).
[b] Eq. (40).

mated from Wyngaard and Coté's (1971) results using a value of

$$\frac{\kappa z}{u_* T_*^2}\frac{\partial}{\partial z}\overline{w\theta^2} = \frac{\kappa z}{u_* q_*^2}\frac{\partial}{\partial z}\overline{wq^2}$$

of 0.2 for $z/L=-0.1$.

For the humidity variance budget, our results indicate that production is equal to dissipation, with the dissipation determined from the humidity spectrum using $\beta_q=0.50$. Had we used $\beta_q=\beta_\theta=0.41$, the ratio of production to dissipation for humidity variance would have been 0.79, close to that found for temperature variance.

The results for the temperature variance budget are presented in Table 5. Averaged over the four runs, the ratio of production to dissipation is 0.84. If we include the estimated flux divergence term, also a loss, the production rate is 28% less than the sum of dissipation and flux divergence.

There are many factors that could have contributed to this relatively small imbalance. We can rule out instrumental problems, because of the low noise levels, the consistency of the high-frequency data with earlier results, and the good agreement between AFCRL and UCSD fluctuating temperature levels (see Fig. 11). However it is possible, for example, that the small-scale temperature field is slightly anisotropic, so that $\chi_\theta < 6\mathfrak{D}\overline{(\partial\theta/\partial x)^2}$. Evidence of anisotropy, in the form of skewed temperature derivatives, has been widely reported (Mestayer *et al.*, 1976). We also found the skewness of $\partial\theta/\partial t$ to be non-zero, with typical values of −0.7.

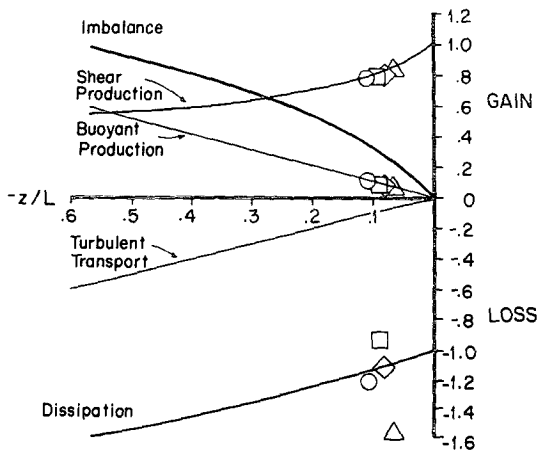

FIG. 10. The dimensionless turbulent kinetic energy budget components versus $-z/L$. The solid lines are from Wyngaard and Coté (1971). Run 1, circles; run 2, squares; run 3, diamonds; run 4, triangles.

TABLE 4. Humidity variance budget equation terms.

Run	$-2\overline{wq}\frac{\partial Q}{\partial z}$ [a] (10^2 g^2 m^{-6} s^{-1})	χ_q (10^2 g^2 m^{-6} s^{-1})	$\frac{\partial \overline{wq^2}}{\partial z}$ [b] (10^2 g^2 m^{-6} s^{-1})	$\frac{-2\overline{wq}\frac{\partial Q}{\partial z}}{\chi_q}$	$-2\overline{wq}\frac{\partial Q}{\partial z}$ [c] (10^2 g^2 m^{-6} s^{-1})
1	0.97	1.18	0.18	0.82	1.37
2	1.29	1.10	0.24	1.17	1.74
3	1.37	1.10	0.24	1.25	1.80
4	0.68	0.91	0.12	0.75	0.86
Average	1.08	1.07	0.20	1.01	1.44

[a] Eq. (22).
[b] Wyngaard and Coté (1971).
[c] Neglecting stability effects.

The mean temperature gradient contribution to the temperature variance production term was not measured directly, but was estimated from Eq. (18), with $\kappa=0.35$ and $\alpha_T=1.35$. We also tried the Hicks and Dyer (1972) formulation

$$\varphi_T = \frac{1}{\alpha_T}(1-15z/L)^{-\frac{1}{2}} \tag{41}$$

with $\alpha_T=1.0$ and $\kappa=0.41$. This gave virtually identical production rates.

The flux divergence term was also not measured directly, but was taken from Wyngaard and Coté's (1971) results. Their data were quite scattered, however, rendering our estimates here somewhat uncertain.

TABLE 5. Temperature variance budget equation terms.

Run	$-2\overline{w\theta}\frac{\partial T}{\partial z}$ [a] (10^3 K^2 s^{-1})	χ_θ (10^3 K^2 s^{-1})	$\frac{\partial \overline{w\theta^2}}{\partial z}$ [b] (10^3 K^2 s^{-1})	$\frac{-2\overline{w\theta}\frac{\partial T}{\partial z}}{\chi_\theta}$	$-2\overline{w\theta}\frac{\partial T}{\partial z}$ [c] (10^3 K^2 s^{-1})
1	4.80	6.41	0.91	0.75	6.77
2	3.61	3.82	0.66	0.94	4.87
3	2.21	2.18	0.39	1.01	2.91
4	1.56	2.33	0.27	0.67	1.98
Average	3.04	3.68	0.56	0.84	4.13

[a] Eq. (18).
[b] Wyngaard and Coté (1971).
[c] Neglecting stability effects.

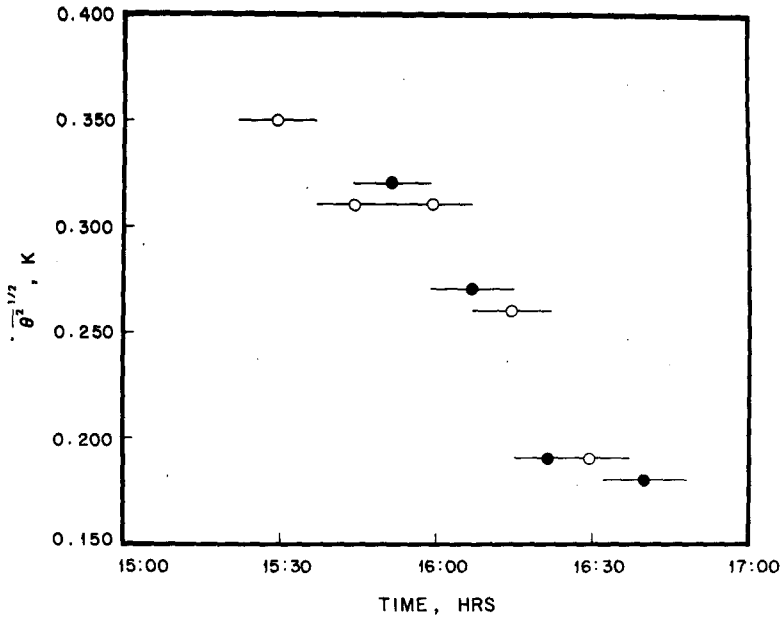

FIG. 11. Values of the rms temperature fluctuations during the experiment. AFCRL (open circles), UCSD (solid circles).

Finally, we should mention that we used a horizontally homogeneous, stationary model of the temperature variance budget, and neglected radiation effects. From the work of Townsend (1958), Brutsaert (1972) and Coantic (1975), the radiation effects can be expected to be an order of magnitude smaller than our imbalance and of the opposite sign. Similarly, the observations of $\partial\overline{\theta^2}/\partial t$ (see Fig. 11) show it is of the same sign as the imbalance but an order of magnitude smaller. Inhomogeneity effects are more difficult to assess, but following the arguments of Wyngaard and Coté (1971) one can show that very large horizontal gradients in $\overline{\theta^2}$ (100% change in less than 1 km) or mean temperature (5 K km^{-1}) would be required to account for the imbalance. While (described in Section 3a) the soil was drying out during the runs, with some areas of standing water, it seems unlikely that this would have caused such strong inhomogeneity.

Thus while the causes for the temperature variance budget imbalance cannot be precisely identified, it seems likely that there could be a number of contributors.

d. Flux estimates neglecting stability effects

To determine the effect of neglecting stability, the fluxes were estimated using the expressions strictly valid only under neutral conditions. Thus Eq. (4) was used to estimate stress, and T_* and q_* were found from

$$T_* = -\left(\frac{\kappa z \chi_\theta \alpha_T}{2u_*}\right)^{\frac{1}{2}}, \tag{42}$$

$$q_* = -\left(\frac{\kappa z \chi_q \alpha_q}{2u_*}\right)^{\frac{1}{2}}. \tag{43}$$

These flux estimates also agreed well with the direct measurements, in spite of the neglect of stability effects. The stress estimate was 16% high, compared with the 6% overestimate (Table 2) with stability effects included. Heat flux was 3% low, compared with 12% high; and moisture flux was 10% low, compared with 2% high.

To investigate this apparent anomaly further, we calculated the magnitudes of the discarded stability contributions to the u_*^2 estimate. Combining Eqs. (9) and (12) yields

$$u_*^2 = (\kappa z \epsilon)^{\frac{2}{3}}\left(1+\frac{I}{\epsilon}\right)^{\frac{2}{3}}\left(1-15\frac{z}{L}\right)^{1/6}. \tag{44}$$

From Table 3, values of I_m/ϵ and $-z/L_m$ were used to compute the last two factors in (44). It was found that their product was nearly unity even though the individual terms themselves were substantially different from unity. Thus although the simplified Eq. (4) gave good estimates of the momentum flux, one must be cautious in drawing the conclusion that stability effects are negligible. For example, the above could lead to the conclusion that shear production and dissipation are in balance, which is clearly not the case in unstable conditions.

5. Conclusions

The estimates of the momentum, heat and moisture fluxes from the dissipation techniques agree well with those measured directly.

The turbulent kinetic energy budget was found to agree with that presented by Wyngaard and Coté (1971) for unstable conditions. Viscous dissipation, the largest term, is balanced by shear production and an imbalance (presumably pressure transport) term. The production and dissipation terms in the humidity variance budget were found essentially in balance, which agrees with Wyngaard and Coté's temperature variance budget results if $\beta_q = 0.50$.

The present experiment is apparently the first in which the dissipation rate of temperature variance was directly measured simultaneously with $\overline{w\theta}$ and other variables which permitted estimation of its production rate. The average ratio of production to dissipation was 0.84. Together with the behavior of the flux divergence term, estimated from Wyngaard and Coté (1971), these results imply a slightly imbalanced temperature variance budget. Possible reasons for the imbalance are considered but none can be definitely identified as a significant contributor.

The one-dimensional spectra of the streamwise velocity fluctuations and temperature fluctuations, presented in Kolmogorov-normalized form, compare favorably with the results of Williams (1974). Values of the universal constants of $\alpha_1 = 0.50 \pm 0.02$ and $\beta_\theta = 0.41 \pm 0.02$ were obtained. The deviations from Taylor's hypothesis caused by high turbulence levels were found to have significant effects on the values of α_1 and β_θ and the dissipation rates ϵ and χ_θ.

Acknowledgments. We would like to thank D. A. Haugen and J. C. Kaimal for their cooperation and work in the experiment. We would also like to thank T. K. Deaton for his efforts in designing and constructing the special electronic circuits that made the experiment a success, as well as for his work during the experiment.

Acknowledgments are also due to J. L. Way who designed the digital data acquisition system and to R. A. Stanford and K. N. Helland who wrote most of the computer programs used in the data reduction.

We would like to thank M. Coantic, S. McConnell, C. A. Paulson, K. F. Schmitt, R. B. Williams, R. M. Williams and R. Hill for valuable comments on an earlier version of the paper.

We are also grateful to B. Hanson and J. Trebing for patiently and expertly typing several drafts of this paper.

The field experiment was performed under ARPA Contract USA-DAHCO 4-72-C-0037 and AFOSR Grant 72-2287. Data reduction and analysis were made while the authors were supported by the following contracts and grants: FHC (AFOSR Grant 72-2287), CAF (NSF/IDOE 14055; NSF OCD 74-22471; ONR N00014-75-C-0152), JLR (NSF ENG 74-14408; NSF OCD 74-22471).

REFERENCES

Busch, N. E., and H. A. Panofsky, 1968: Recent spectra of atmospheric turbulence. *Quart. J. Roy. Meteor. Soc.*, **94**, 132–140.

Brutsaert, W., 1972: Radiation, evaporation and the maintenance of turbulence under stable conditions in the lower atmosphere. *Bound.-Layer Meteor.*, **2**, 309–325.

Businger, J. A., J. C. Wyngaard, Y. Izumi and E. F. Bradley, 1971: Flux-profile relationships in the atmospheric surface layer. *J. Atmos. Sci.*, **28**, 181–189.

Coantic, M., 1975: An *Introduction to Turbulence in Geophysics and Air-Sea Interactions*. Course notes, University of California, San Diego, 283 pp.

Corrsin, S., 1964: Further generalization of Onsager's cascade model for turbulence spectra. *Phys. Fluids*, **7**, 1156–1159.

Deacon, E. L., 1959: The measurement of turbulent transfer in the lower atmosphere. *Advances in Geophysics*, Vol. 6, Academic Press, 211–228.

Dyer, A. J., 1975: Measurement of turbulent fluxes by fluxatron and NIFTI technique. *Atmos. Tech.*, **7**, 24–29.

——, 1967: The turbulent transport of heat and water vapor in an unstable atmosphere. *Quart. J. Roy. Meteor. Soc.*, **93**, 501–508.

Elliott, J. A., 1975: The measurement of pressure fluctuations in the atmospheric boundary layer. *Atmos. Tech.*, **7**, 30–32.

Garratt, J. R., 1972: Studies of turbulence in the surface layer over water (Lough Neagh). Part II. Production and dissipation of velocity and temperature fluctuations. *Quart. J. Roy. Meteor. Soc.*, **98**, 642–657.

Gibson, C. H., and R. B. Williams, 1969: Turbulence structure in the atmospheric boundary layer over the open ocean. *Proc. AGARD Conf. Aerodynamics of Atmospheric Shear Flows*, Vol. 48, 5–1 to 5–9.

——, G. R. Stegen and R. B. Williams, 1970: Statistics on the finestructure of turbulent velocity and temperature fields measured at high Reynolds number. *J. Fluid Mech.*, **41**, 153–167.

Haugen, D. A., J. C. Kaimal and E. F. Bradley, 1971: An experimental study of Reynolds stress and heat flux in the atmospheric surface layer. *Quart. J. Roy. Meteor. Soc.*, **97**, 168–180.

Heskestad, G., 1965: A generalized Taylor hypothesis with application for high Reynolds number turbulent shear flows. *J. Appl. Mech.*, **87**, 735–740.

Hicks, B. B., and A. J. Dyer, 1972: The spectral density technique for the determination of eddy fluxes. *Quart. J. Roy. Meteor. Soc.*, **98**, 838–844.

Hinze, J. O., 1959: *Turbulence*. McGraw-Hill, 586 pp.

Kaimal, J. C., 1975: Sensors and techniques for direct measurement of turbulent fluxes and profiles in the atmospheric surface layer. *Atmos. Tech.*, **7**, 7–14.

——, and D. A. Haugen, 1969: Some errors in the measurement of Reynolds stress. *J. Appl. Meteor.*, **8**, 460–462.

——, J. C. Wyngaard, D. A. Haugen, O. R. Coté, Y. Izumi, S. J. Caughey and C. J. Readings, 1976: Turbulence structure in the convective boundary layer. *J. Atmos. Sci.* (in press).

LaRue, J. C., T. Deaton and C. H. Gibson, 1975: Measurement of high-frequency turbulent temperature. *Rev. Sci. Instrum.*, **46**, 757–764.

Leavitt, E., and C. A. Paulson, 1975: Statistics of surface layer turbulence over the tropical ocean. *J. Phys. Oceanogr.*, **5**, 143–156.

Lumley, J. L., 1965: Interpretation of time spectra measured in high-intensity shear flows. *Phys. Fluids*, **8**, 1056–1062.

McBean, G. A., 1972: Instrument requirements for eddy correlation measurements. *J. Appl. Meteor.*, **11**, 1978–1084.

——, R. W. Stewart and M. Miyake, 1971: The turbulent energy budget near the surface. *J. Geophys. Res.*, **76**, 6540–6549.

——, and J. A. Elliott, 1975: The vertical transports of kinetic energy by turbulence and pressure in the boundary layer. *J. Atmos. Sci.*, **32**, 753–766.

Mestayer, P. G., C. H. Gibson, M. F. Coantic and A. S. Patel, 1976: Local anisotropy in heated and cooled turbulent boundary layers. *Phys. Fluids*, **19**, 1279–1287.

Miyake, M., M. Donelan, G. McBean, C. Paulson, F. Badgley and E. Leavitt, 1970: Comparison of turbulent fluxes over water determined by profile and eddy correlation techniques. *Quart. J. Roy. Meteor. Soc.*, **96**, 132–137.

Monji, N., 1973: Budgets of turbulent energy and temperature variance in the transition zone from forced to free convection. *J. Meteor. Soc. Japan*, **51**, 133–145.

Pao, Y. H., 1965: Structure of turbulent velocity and scalar fields at large wavenumbers. *Phys. Fluids*, **8**, 1063–1075.

Paquin, J. E., and S. Pond, 1971: The determination of the Kolmogoroff constants for velocity, temperature and humidity fluctuations from second- and third-order structure functions. *J. Fluid Mech.*, **50**, 257–269.

Pond, S., R. W. Stewart and R. W. Burling, 1963: Turbulence spectra in the wind over waves. *J. Atmos. Sci.*, **20**, 319–324.

——, G. T. Phelps, J. E. Paquin, G. McBean and R. W. Stewart 1971: Measurements of the turbulent fluxes of momentum, moisture and sensible heat over the ocean. *J. Atmos. Sci.*, **28**, 901–917.

Readings, C. J., D. A. Haugen and J. C. Kaimal, 1974: The 1973 Minnesota atmospheric boundary layer experiment. *Weather*, **29**, 309–312.

Smith, S. D., 1967: Thrust-anemometer measurements of wind-velocity spectra and of Reynolds stress over a coastal inlet. *J. Mar. Res.*, **25**, 239–262.

——, 1970: Thrust-anemometer measurements of wind turbulence, Reynolds stress and drag coefficient over the sea. *J. Geophys. Res.*, **75**, 6758–6770.

Stegen, G. R., C. H. Gibson and C. A. Friehe, 1973: Measurements of momentum and sensible heat fluxes over the open ocean. *J. Phys. Oceanogr.*, **3**, 86–92.

Taylor, G. I., 1938: The spectrum of turbulence. *Proc. Roy. Soc. London*, **A164**, 476–490.

Taylor, R. J., 1961: A new approach to the measurement of turbulent fluxes in the lower atmosphere. *J. Fluid Mech.*, **10**, 449–458.

Tennekes, H., and J. C. Wyngaard, 1972: The intermittent small-scale structure of turbulence: data-processing hazards. *J. Fluid Mech.*, **55**, 93–103.

Townsend, A. A., 1958: The effects of radiative transfer on turbulent flow in a stratified fluid. *J. Fluid Mech.*, **4**, 361–375.

Weiler, H. S., and R. W. Burling, 1967: Direct measurements of stress and spectra of turbulence in the boundary layer over the sea. *J. Atmos. Sci.*, **24**, 653–664.

Williams, R. M., Jr., 1974: High frequency temperature and velocity fluctuations in the atmospheric boundary layer. Ph.D. thesis, Oregon State University, 81 pp.

Wyngaard, J. C., 1968: Measurement of small-scale turbulence structure with hot wires. *J. Sci. Instrum.*, **1**, 1105–1108.

——, 1969: Spatial resolution of the vorticity meter and other hot-wire arrays. *J. Sci. Instrum.*, **2**, 983–987.

——, 1971: Spatial resolution of a resistance wire temperature sensor. *Phys. Fluids*, **14**, 2052–2054.

——, 1972: The effect of velocity sensitivity on temperature derivative statistics in isotropic turbulence. *J. Fluid Mech.*, **48**, 763–769.

——, and O. R. Coté, 1971: The budgets of turbulent kinetic energy and temperature variance in the atmospheric surface layer. *J. Atmos. Sci.*, **28**, 190–201.

——, and Y. H. Pao, 1971: Some measurements of the fine structure of large Reynolds number turbulence. *Statistical Models and Turbulence*, M. Rosenblatt and C. Van Atta, Eds., Springer-Verlag, 384–401.

——, and S. F. Clifford, 1976: Taylor's hypothesis and high-frequency turbulence spectra. Submitted to *J. Atmos. Sci.*